

X-Ray Diffraction Measurement of the Effect of Layer Thickness on the Ferroelectric Transition in Epitaxial $\text{KTaO}_3/\text{KNbO}_3$ Multilayers

E. D. Specht,* H.-M. Christen,^{†,‡} D. P. Norton,[†] and L. A. Boatner[†]

Oak Ridge National Laboratory, Oak Ridge, Tennessee 37831-6118

(Received 17 November 1997)

$\text{KTaO}_3/\text{KNbO}_3$ strained-layer superlattices of variable periodicity were grown by pulsed laser deposition on KTaO_3 substrates. The KNbO_3 layers were found to be strained in plane to match the substrate lattice parameter. Therefore, the applied strain is independent of the layer thickness. High-temperature x-ray diffraction was used to measure the ferroelectric-paraelectric phase transition temperature T_c . For superlattice periodicity $\Lambda \leq 5.1$ nm, $T_c = 475$ K, independent of Λ . For $\Lambda > 5.1$ nm, T_c increases to 825 K at $\Lambda = 33.8$ nm. [S0031-9007(98)06010-4]

PACS numbers: 77.80.Bh, 61.10.Eq, 77.84.Dy

Many attempts have been made to measure the effects of sample size on the paraelectric-ferroelectric phase transition, almost all involving BaTiO_3 . Fine particles of BaTiO_3 have been found to have a depressed transition temperature. While bulk BaTiO_3 has a Curie temperature $T_c = 403$ K, T_c falls below room temperature for a crystallite size below a critical value variously reported as 25 to 200 nm. It is unclear whether this is an intrinsic effect of particle size or an artifact of the structural and chemical differences between large BaTiO_3 crystals and small particles. For example, the small, highly defective crystallites simultaneously show increased particle size, reduced defects, and increased T_c , all at the same annealing temperature (see Ref. [1] for a summary). Other polycrystalline systems exhibit similarly variable results [2–4].

Thin films, on the other hand, can be annealed to high temperature to remove defects while retaining small film thickness. While epitaxial BaTiO_3 films between 6.7 and 400 nm in thickness have been analyzed, interpretation has been complicated by residual stress, and there is no clear evidence of a phase transition [5,6]. Tabata *et al.* observe broad anomalies in the dielectric constant of $\text{BaTiO}_3/\text{SrTiO}_3$ multilayers, but not a clear phase transition [7]. They infer that a phase transition occurs at “high temperature,” but do not report the variation of T_c with layer thickness. The misfit between (100) SrTiO_3 and (001) BaTiO_3 is 2.3%. For layers thinner than about 4 nm, Tabata *et al.* find that the layers grow with equal in-plane lattice parameters, so residual stress is high, but uniform. For greater thicknesses, BaTiO_3 and SrTiO_3 grow with different lattice parameters, introducing strain variations through their thicknesses [7]. For these thicker layers, it is understandable that inhomogeneous strain leads to broadening of the phase transition. It is curious that the transition is broadened in the thinner layers.

In the best-controlled prior study of ferroelectric films, a phase transition has been reported in epitaxial $(\text{Ba}, \text{Sr})\text{TiO}_3$ grown on MgO by Zakharchenko *et al.* A broadened transition was observed, with T_c increasing as film thickness is increased from 0.26 to 2.1 μm , an

increase which Zakharchenko *et al.* attribute entirely to changes in residual stress [8].

We have used $\text{KTaO}_3/\text{KNbO}_3$ strained-layer superlattices of variable periodicity to isolate the effect of layer thickness. Bulk KTaO_3 is paraelectric at all temperatures [9], while bulk KNbO_3 is ferroelectric below $T_c = 708$ K [10]. Because the lattice mismatch is below 0.5%, the intrinsic effects of film thickness may be studied without the influence of large strains. The large total thickness of the superlattice produces the sharp diffraction peaks needed for accurate lattice parameter measurements. We demonstrate that each layer is below the critical thickness for the formation of misfit dislocations, so the in-plane lattice parameter of the entire multilayer is the same as that of the substrate. Stress is homogeneous and independent of layer thickness. Interfaces are commensurate, with a minimum level of defects. This leaves film thickness as the primary cause of variation in properties.

KTaO_3 and KNbO_3 layers were grown on KTaO_3 (100) substrates by pulsed laser deposition as described in Ref. [11]. Each film was grown to the same total thickness of 170 nm, consisting of alternating layers of KNbO_3 and KTaO_3 with a superlattice periodicity Λ of 0.8 to 33.8 nm. The KNbO_3 and KTaO_3 layers were of nominally equal thickness, as calibrated by transmission electron microscopy (TEM) [12], and the bilayer thickness was determined by high-angle x-ray diffraction as described below. The films are flat, with atomically sharp interfaces [12]. The mosaic spread of the film, determined by x-ray diffraction, is $\sim 0.05^\circ$, indicating excellent crystal quality and epitaxy. For comparison, a 170 nm film of $\text{K}_{0.5}\text{Ta}_{0.5}\text{Nb}_{0.5}\text{O}_3$ was grown by codeposition from a rotating target containing both KTaO_3 and KNbO_3 as described in Ref. [13].

The structure of these thin KNbO_3 layers differs qualitatively from thicker KNbO_3 films. Very thick (1.5 μm) films have the bulk structure: an orthorhombic cell with $a = 0.5495$ nm, $b = 0.5721$ nm, and $c = 0.3974$ nm. Intermediate films (166 nm) are still orthorhombic, but with $a = 0.3975$ nm, $b = 0.4001$ nm,

and $c = 0.4055$ nm [11]. The layers treated in this work, 0.37 to 16.9 nm in thickness, do not exhibit the split peaks of orthorhombic structures. The observed peaks are consistent with a tetragonal structure, with (001) normal to the surface and [100] aligned with the substrate [100].

A Cu source was used for x-ray diffraction measurements, with Ge(111) crystals as monochromator and analyzer. Slits selected the $K_{\alpha 1}$ line. Radial (θ - 2θ) scans were taken through the KTaO_3 and KNbO_3 (002) and (202) Bragg peaks to determine in-plane and out-of-plane lattice parameters. Multiple film reflections are observed (Fig. 1), so the peaks can be indexed and the superlattice periodicity Λ accurately determined. For the film with the thinnest layers, only the fundamental reflection was clearly observed, so $\Lambda = 0.8$ nm was determined by assuming the same growth rate as the other multilayers. These measurements of peak position do not, however, give any information concerning either the relative thickness of the two layers or the atomic layer spacing in either material; these will affect only the intensities of the reflections.

T_c was measured by monitoring changes in lattice constant as the sample was heated in vacuum. Results are shown in Fig. 2. For the KTaO_3 substrate, and the codeposited $\text{KTa}_{0.5}\text{Nb}_{0.5}\text{O}_3$ film, we measure plane spacings d_{002} and d_{202} and calculate the out-of-plane lattice parameter $c = 2d_{002}$ and the in-plane lattice parameter $a = 2/\sqrt{d_{202}^{-2} - d_{002}^{-2}}$. For the superlattices, we choose superlattice (00 l) and (20 l) reflections and calculate the superlattice periodicity $\Lambda = ld_{00l}$ and the in-plane lattice parameter $a = 2/\sqrt{d_{20l}^{-2} - d_{00l}^{-2}}$. We plot the thermal expansion of Λ along with the absolute values of a and c in order to facilitate comparison of thermal expansion in films with different Λ .

For all films, the in-plane film lattice parameters match the substrate's to within 0.05%. Data for only the extreme values of Λ are plotted (Fig. 2). The films are below the critical thickness for the nucleation of misfit dislocations,

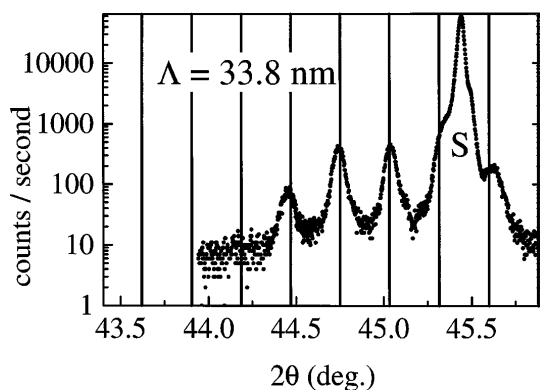


FIG. 1. Radial scan through the (002) Bragg peaks for superlattices with $\Lambda = 33.8$ nm. Gridlines indicate calculated superlattice peak positions. "S" indicates the substrate (002) peak.

so all films are homogeneously and equally strained, and any differences in the ferroelectric behavior can be attributed to the differing layer thicknesses.

At high temperatures, the out-of-plane thermal expansion of the film is similar to that of the substrate. At lower temperatures, the thermal expansion changes sign; this anomalous behavior signals the paraelectric to ferroelectric phase transition. Some rounding of the transition is evident, which we attribute to nonuniformity in layer thickness. No hysteresis is observed; behavior is the same on warming and cooling. T_c is taken as the highest temperature where thermal expansion changes sign and is plotted in Fig. 3(a).

Because the substrate is insulating, electronic measurements to confirm the ferroelectric character of the phase transition will require deposition of interdigitated electrodes. This has not yet been performed. We note, however, that bulk KNbO_3 and $\text{KNb}_{0.5}\text{Ta}_{0.5}\text{O}_3$ exhibit similar transitions from a cubic paraelectric to a tetragonal ferroelectric phase at 708 K [10] and 373 K [14], respectively. In the limit $\Lambda \rightarrow \infty$, each KNbO_3 layer should approach bulk behavior, subject to an in-plane compressive strain of 0.5% in the cubic phase. In the limit $\Lambda \rightarrow 0$, the film has a uniform composition of $\text{KNb}_{0.5}\text{Ta}_{0.5}\text{O}_3$, and again should exhibit bulk behavior, now with an in-plane compressive strain of 0.2%. The observed dependence of thermal expansion on layer thickness is consistent in both

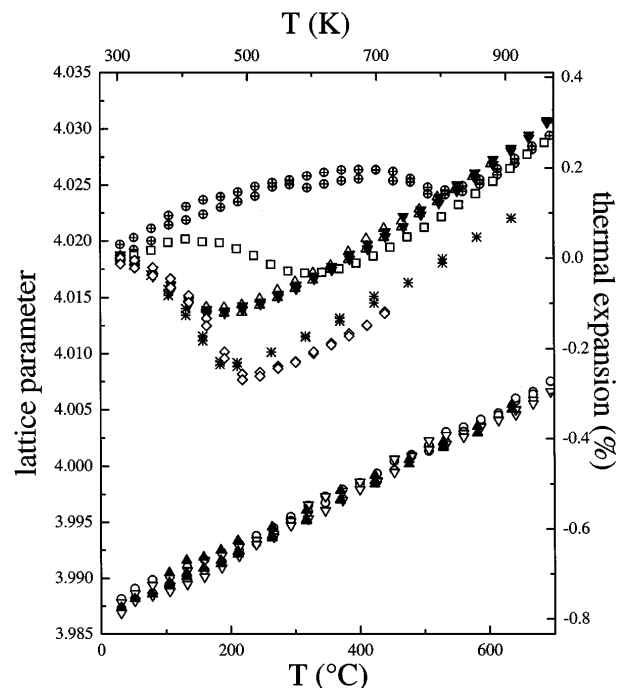


FIG. 2. Temperature dependence of the lattice parameter of a KTaO_3 substrate (\circ), of the in-plane lattice parameter of codeposited $\text{KTa}_{0.5}\text{Nb}_{0.5}\text{O}_3$ (\blacktriangle) and a $\Lambda = 34$ nm multilayer (∇), and of the out-of-plane lattice parameters of codeposited $\text{KTa}_{0.5}\text{Nb}_{0.5}\text{O}_3$ ($*$), and multilayers with $\Lambda = 33.8$ nm (\oplus), 10.2 nm (\square), 4.8 nm (\triangle), 3.15 nm (\blacktriangledown), and 0.8 nm (\diamond).

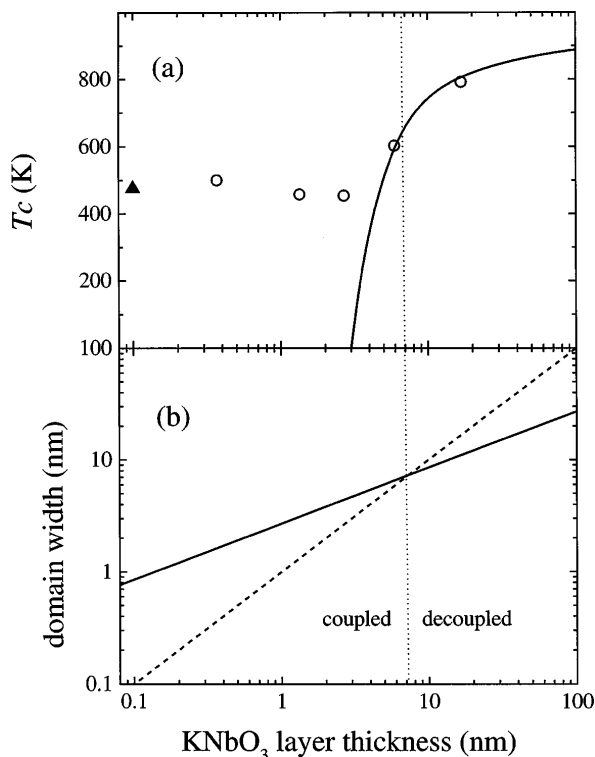


FIG. 3. (a) Curie temperature of multilayer films (\circ) and of codeposited $\text{KTA}_{0.5}\text{Nb}_{0.5}\text{O}_3$ (\blacktriangle), which has been arbitrarily drawn at a thickness of 0.1 nm. Solid line: T_c calculated by [16], using $\xi = 1.8$ nm and $T_{c\infty} = 900$ K. (b) Solid line: ferroelectric domain width, calculated by [16], using $\xi = 1.8$ nm and $T_{c\infty} = 900$ K. Dashed line: separation between KNbO_3 layers. Well to the left of the dotted line, layer separation \ll domain width, and layers are strongly coupled. Well to the right, layer separation \gg domain width and layers are decoupled.

limits with a bulklike phase transition, where the tetragonal ferroelectric phase is constrained by the substrate to domains with c parallel or antiparallel to the surface normal.

Stress and defects at interfaces might cause either a depression or elevation in T_c . Because we have grown films with no misfit dislocations on a structurally and chemically similar substrate, we expect few defects and a homogeneous stress state; TEM confirms this expectation [11]. The remaining, intrinsic effect of small layer thickness is to depress T_c . As first described for ferromagnetic films [15], the free energy density of a film of thickness t with polarization P in parallel domains of width D parallel and antiparallel to the surface normal is

$$F = F_{\text{bulk}}(T) + \frac{\sigma_{\text{wall}}}{D} + \frac{0.85P^2D}{t}, \quad (1)$$

where the three terms represent bulk, domain wall, and surface contributions, respectively. As t is decreased, the free energy of the ferroelectric phase is increased relative to the paraelectric, lowering T_c . $D \sim \sqrt{t}$ as domain size shrinks to reduce the surface energy.

Wang *et al.* [16] have performed detailed numerical calculations, including effects such as nonzero domain wall width and surface depolarization which are not included in Eq. (1). Using a phenomenological model for the ferroelectric, Wang *et al.* calculate $T_c/T_{c\infty}$ as a function of t/ξ , where ξ is the ferroelectric correlation length, which corresponds to the width of a domain wall, and $T_{c\infty}$ is the transition temperature of a thick film. The thickness dependence of T_c depends only on these two parameters. The small amount of data precludes a verification of the temperature dependence predicted by Wang *et al.* If we assume that their result applies to the thicker multilayers, we find that $\xi \sim 1.8$ nm and $T_{c\infty} \sim 900$ K [Fig. 3(a)]. This model clearly does not fit the thinner layers, as we shall discuss below.

The model of Wang *et al.* assumes a second-order phase transition. The transition for bulk KNbO_3 is first order, becoming second order for bulk $\text{KTA}_x\text{Nb}_{1-x}$ solid solutions [14]. It can be seen from Fig. 2 that the lattice parameter varies continuously through the observed phase transition, so it appears that this assumption applies to these films, perhaps due to the effects of stress or thickness. The model further assumes that the films are surrounded by vacuum, while the observed KNbO_3 layers are surrounded by KTAO_3 . The use of KTAO_3 has practical advantages over vacuum. The interfaces remain clean, and due to the pseudomorphic growth, the interfaces preserve the bulk structure. However, the dielectric response of KTAO_3 will reduce the surface term in Eq. (1) and raise T_c for thin layers.

$T_{c\infty}$ is elevated considerably from the 708 K transition temperature of unstressed KNbO_3 . Near the phase transition in the films, the misfit between bulk KNbO_3 and KTAO_3 is 0.5% in the paraelectric phase but only 0.35% in the ferroelectric phase, so the applied stress will stabilize the ferroelectric phase. We are not aware of a detailed model of the phase transition of KNbO_3 which could be used to confirm that the elevated Curie temperature is due to the applied stress. We can, however, compare the results to those obtained for the structurally and phenomenologically similar BaTiO_3 . Using a phenomenological model of the phase transition for BaTiO_3 , it has been calculated [8] that the fractional increase in T_c brought about by a compressive in-plane strain ε is $\Delta T_c/T_c = 120\varepsilon$. We observe a comparable increase of $\Delta T_c/T_c = 54\varepsilon$ for KNbO_3 .

Two effects compete as the layers become thinner. Because the ferroelectric layers are closer together, they will interact more strongly. At the same time, the width of the ferroelectric domains will decrease to minimize the free energy [Eq. (1)]. This weakens the interaction between layers: Since the field produced by domains of width D falls off (to leading order) as $\exp(-Dz)$ with distance normal to the layers z , layers will interact strongly when separated by less than a domain width. Figure 3(b) compares the calculated domain width [16] to layer

spacing. For layer thicknesses much less than 7 nm, layers are strongly coupled; these short-wavelength superlattices behave in the same way as alloyed films. For much larger thicknesses, the layers are decoupled and follow the single-layer calculations of Wang *et al.* [16]. Further calculations will be required to determine whether the crossover behavior can be accounted for by simple models based on Eq. (1). Our estimate of ξ and $T_{c\infty}$ assumes an abrupt crossover from thin to thick-layer behavior; if the crossover is more gradual, these parameters may be very different. Future experiments will independently vary the spacing and thickness of ferroelectric layers to distinguish these competing effects.

It can be seen from Fig. 2 that the expansion associated with the onset of ferroelectricity is greater for the codeposited mixture and the shortest-period multilayer than for the longer-period multilayers. Changes in T_c and of lattice expansion do not correlate. The large depression in T_c occurs between $\Lambda = 33.8$ and $\Lambda = 4.8$ nm; the expansion is unchanged over this range. The expansion increases as Λ decreases from 3.15 to 0.8 nm, where T_c does not change. This suggests that the changes in the lattice expansion are due to local effects, while T_c is controlled by longer-range electrostatic interactions. In particular, all Ta and Nb atoms occupy neighboring sites only for the $\Lambda = 0.8$ nm multilayer; for the others most neighboring sites are occupied by the same element.

To conclude, we have used strained-layer superlattices to study the variation of T_c with layer thickness and layer separation without confounding changes in strain. Layer thickness and separation are kept equal; future experiments will study their effects independently. While similarly grown $\text{BaTiO}_3/\text{SrTiO}_3$ multilayers show only a broad anomaly [7], we find a clear phase transition. This may be an effect of the much lower misfit (0.5% in $\text{KNbO}_3/\text{KTaO}_3$, 2.3% in $\text{BaTiO}_3/\text{SrTiO}_3$). Alternatively, it may be that the transition appears more sharply in the thermal expansion than in dielectric constant measurements; future measurements of dielectric constant in $\text{KNbO}_3/\text{KTaO}_3$ multilayers will give a more direct comparison between the systems. Even in $\text{KNbO}_3/\text{KTaO}_3$, the effects of strain are large: $T_c = 813$ K for the thickest layers, while $T_c = 708$ K in bulk KNbO_3 . However, because the in-plane lattice parameter is locked to that of the substrate, strain is independent of layer thickness. While

interlayer coupling prevents T_c from falling below 450 K, extrapolation suggests that ferroelectricity in KNbO_3 disappears (i.e., $T_c = 0$) for thicknesses near 3 nm.

We thank Fred Walker for helpful discussions and Mike Urbanik for polishing the substrates. This research was sponsored by the Division of Materials Sciences, U.S. Department of Energy under Contract No. DE-AC05-96OR22464 with Lockheed Martin Energy Research Corporation.

*Metals and Ceramics Division. Internet: esy@ornl.gov.

†Solid State Division.

‡Present address: Neocera, 10000 Virginia Manor Road Suite 300, Beltsville, MD 20705-4215.

- [1] F.-S. Yen, H.-I. Hsiang, and Y.-H. Chang, *Jpn. J. Appl. Phys.* **34**, 6149 (1995).
- [2] A. Hadni and R. Thomas, *Thin Solid Films* **81**, 247 (1981).
- [3] A. Hadni and R. Thomas, *Ferroelectrics* **59**, 221 (1984).
- [4] J.F. Scott, H.M. Duiker, P.D. Beale, B. Pouligny, K. Dimmler, M. Parris, D. Butler, and S. Eaton, *Physica (Amsterdam)* **150B**, 160 (1988).
- [5] Y. Yoneda, K. Kasatani, H. Terauchi, Y. Yano, T. Terashima, and Y. Bando, *J. Phys. Soc. Jpn.* **62**, 1840 (1993).
- [6] H. Terauchi, Y. Watanabe, H. Kasatani, K. Kamigaki, Y. Yano, T. Terashima, and Y. Bando, *J. Phys. Soc. Jpn.* **61**, 2194 (1992).
- [7] H. Tabata, H. Tanaka, and T. Kawai, *Appl. Phys. Lett.* **65**, 1970 (1994).
- [8] I.N. Zakharchenko, E.S. Nikitin, V.M. Mukhortov, Y.I. Golovko, M.G. Radchenko, and V.P. Dudkevich, *Phys. Status Solidi (a)* **114**, 559 (1989).
- [9] U. T. Höchli, H.E. Weibel, and L. A. Boatner, *Phys. Rev. Lett.* **39**, 1158 (1977).
- [10] E. A. Wood, *Acta Crystallogr.* **4**, 353 (1951).
- [11] H.-M. Christen, L. A. Boatner, J.D. Budai, M.H. Chisholm, L. A. Géa, P.J. Marrero, and D.P. Norton, *Appl. Phys. Lett.* **68**, 1488 (1996).
- [12] H.-M. Christen, E.D. Specht, D.P. Norton, M.F. Chisholm, and L. A. Boatner (to be published).
- [13] H.-M. Christen, D.P. Norton, L. A. Géa, and L. A. Boatner, *Thin Solid Films* (to be published).
- [14] S. Triebwasser, *Phys. Rev.* **114**, 63 (1958).
- [15] C. Kittel, *Phys. Rev.* **70**, 965 (1946).
- [16] Y.G. Wang, W.L. Zhong, and P.L. Zhang, *Phys. Rev. B* **51**, 5311 (1995).